# Offspring of rats with cerebral hypoxia-ischemia manifest cognitive dysfunction in learning and memory abilities

Lu-Lu Xue[1, 3, #], Fang Wang[4, #], Rui-Ze Niu[5], Ya-Xin Tan[3], Jia Liu[5], Yuan Jin[3], Zheng Ma[3], Zi-Bin Zhang[6], Ya Jiang[5], Li Chen[6], Qing-Jie Xia[6], Jun-Jie Chen[7], Ting-Hua Wang[3, 6, *], Liu-Lin Xiong[1, 2, *]

1 Department of Anesthesiology, Affiliated Hospital of Zunyi Medical University, Zunyi, Guizhou Province, China
2 School of Pharmacy and Medical Sciences, Division of Health Sciences, University of South Australia, Adelaide, Australia
3 Institute of Neuroscience, Kunming Medical University, Kunming, Yunnan Province, China
4 Department of Science and Technology, Kunming Medical University, Kunming, Yunnan Province, China
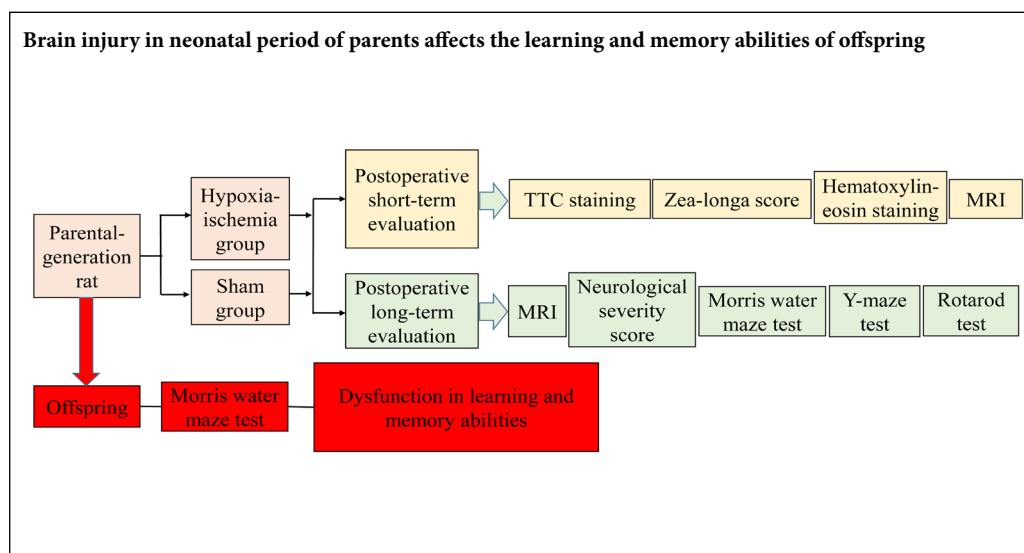5 Department of Laboratory Zoology, Kunming Medical University, Kunming, Yunnan Province, China
6 Institute of Neurological Disease, Department of Anesthesiology, Translational Neuroscience Center, West China Hospital, Sichuan University, Chengdu, Sichuan Province, China
7 Southwest Medical University, Luzhou, Sichuan Province, China

## Graphical Abstract



**Brain injury in neonatal period of parents affects the learning and memory abilities of offspring**

*Correspondence to:*
*Liu-Lin Xiong, MD,*
*499465010@qq.com;*
*Ting-Hua Wang,*
*wangtinghua@vip.163.com.*

*#Both authors contribute equally to this work.*

*orcid:*
*0000-0002-1623-5969*
*(Liu-Lin Xiong)*
*0000-0003-2012-8936*
*(Ting-Hua Wang)*

## Abstract

Neonatal hypoxic-ischemic encephalopathy is a serious neurological disease, often resulting in long-term neurodevelopmental disorders among surviving children. However, whether these neurodevelopmental issues can be passed to offspring remains unclear. The right common carotid artery of 7-day-old parental-generation rats was subjected to permanent ligation using a vessel electrocoagulator. Neonatal hypoxic-ischemic rat models were established by subjecting the rats to 8% $O_2$–92% $N_2$ for 2 hours. The results showed that 24 hours after hypoxia and ischemia, pathological damage, cerebral atrophy, liquefaction, and impairment were found, and Zea-Longa scores were significantly increased. The parental-generation rats were propagated at 3 months old, and offspring were obtained. No changes in the overall brain structures of these offspring rats were identified by magnetic resonance imaging. However, the escape latency was longer and the number of platform crossings was reduced among these offspring compared with normal rats. These results indicated that the offspring of hypoxic-ischemic encephalopathy model rats displayed cognitive impairments in learning and memory. This study was approved by the Animal Care & Welfare Committee of Kunming Medical University, China in 2018 (approval No. kmmu2019072).

*Key Words:* cerebral atrophy; cerebral infarct; cerebral liquefaction; cognitive impairment; magnetic resonance imaging; neonatal brain hypoxia and ischemia; neuronal apoptosis; offspring

*Chinese Library Classification No. R441; R741; Q38*

## Introduction

Neonatal hypoxic-ischemic encephalopathy (HIE), a clinical syndrome associated with neurological dysfunction, is characterized by difficulty initiating and maintaining respiration, disturbed consciousness, decreased muscular tension, pathological reflexes, and seizures. HIE often occurs during the first day of life in term-born and late preterm neonates, with an incidence as high as 1–3% (Graham et al., 2008; Kurinczuk et al., 2010; Selway, 2010; Wachtel and Hendricks-Munoz, 2011). Importantly, 15–20% of affected newborns (1–3 per 1000 full-term births) die during the postnatal period, and an additional 25% will experience severe and permanent neuropsychological sequelae (Vannucci and Perlman, 1997).

Accumulating evidence has demonstrated that HIE could lead to secondary injuries, such as reperfusion injury, edema, increased intracranial pressure, impaired autoregulation, and hemorrhage (Galinsky et al., 2018; Kawarai et al., 2018; Davies et al., 2019), which are known to be pathological mechanisms of neurodevelopmental disorders, such as epilepsy, behavioral deficits, learning disorders, and cerebral palsy (Leviton and Nelson, 1992; Vannucci et al., 1999; Ferriero, 2004; Vannucci and Hagberg, 2004; Sasaoka et al., 2009). Although the underlying pathophysiology of neonatal HIE, including oxidative stress, excitotoxicity, inflammation, and apoptosis (Ferriero, 2004), has been intensively studied, few successful treatments for neonatal HIE have been identified. Hypoxia-ischemia (HI) conditions increase the risks of autism spectrum disorder and attention deficit hyperactivity disorder in children (Driscoll et al., 2018). A previous study demonstrated that prenatal and perinatal complications that cause HI are also associated with an increased risk of autism spectrum disorder (Getahun et al., 2013). Most current studies examining the long-term neurodevelopmental outcomes of HIE have focused on term infants with moderate and severe HIE and have reported increases in the incidence of motor and cognitive neurological disabilities (Mwaniki et al., 2012). The existence of long-term neurodevelopmental disabilities in surviving babies has spontaneously drawn our attention to their offspring. In view of the above-mentioned devastating impacts of HIE on neonatal brain development, whether the offspring of patients with HIE suffer from similar neurological dysfunctions has not been well-examined, although these patients are able and likely to have and raise children. Thus, this question deserves further investigation. This study evaluated the neurobehavioral functions and brain morphologies of HI rat models and detected the neurobehavioral changes in their offspring.

## Materials and Methods

### Animals

Fifty healthy, 7-day-old, specific-pathogen-free, Sprague-Dawley rat pups of both sexes (male/female ratio 1:1), ranging from 12–15 g, were provided by the Department of Zoology of Kunming Medical University, China (license No. K2015-0002). Animal care and all experimental protocols were in strict accordance with the Chinese Experimental Animal Protection and Ethics Committee and the Guidelines for the Care and Use of Laboratory Animals, published by the National Institutes of Health (NIH). The animal protocol was approved in 2018 by the Animal Care & Welfare Committee of Kunming Medical University (approval No. kmmu2019072). All animals were raised with their mothers, in plastic cages, containing softwood, and free access to food and water, at 21–25°C, and humidity of 50–60%.

### Neonatal hypoxic-ischemic brain model establishment and experimental groups

Seven-day-old Sprague-Dawley parental-generation rats were equally and randomly divided into sham group and HI group. All animals were anesthetized by the inhalation of isoflurane (RWD Technology Co., Ltd., Shenzhen, China) and placed in a supine position. Their cervical skin was incised to expose the right common carotid artery, which was subjected to permanent ligation with a vessel electrocoagulator (Spring Medical Beauty Equipment Co., Ltd., Wuhan, China). Sham animals underwent the same procedure, without artery ligation. The neonates were placed onto an electric blanket until awake and returned to their cages with their mothers for 1 hour. The pups were placed in a chamber under a hot lamp, to maintain the temperature at 37°C, and subjected to 8% $O_2$–92% $N_2$ for 2 hours. The air temperature was continuously detected and maintained at 37°C, with humidity at 60–70%. Parental-generation (P) rats were divided into P-Sham and P-HI groups ($n = 6$/group). The P rats were propagated at 3 months old and were housed in standard animal house in a 12-hour light-dark cycle at 21–25°C and air humidity of 50–60% with food and water *ad libitum*. The offspring were divided into Sham-F1 and HI-F1 groups, based on their parent status.

### 2,3,5-Triphenyltetrazolium chloride staining

To identify the establishment of the HI model, P rats were randomly selected for 2,3,5-triphenyltetrazolium chloride (TTC) staining, 24 hours after HI ($n = 5$/group). After anesthesia, the brains were quickly removed and incubated at –20°C for approximately 20 minutes. A 2-mm thick brain tissue section was taken 1 mm behind the olfactory bulb and cut into 4 pieces of equal size and shape. The brain slices were incubated in 2% TTC (Sigma, St Louis, MO, USA), in the dark, at 37°C, for approximately 30 minutes. The slices were washed with phosphate-buffered saline (PBS) and fixed in 4% paraformaldehyde, for approximately 24 hours, for observation and image acquisition. The infarct size was traced and analyzed using ImageJ Software (Version 1.43u; National Institutes of Health, Bethesda, MD, USA). The infarct percentage was calculated as (contralateral hemisphere volume – non-infarct ipsilateral hemisphere volume)/contralateral hemisphere volume × 100. Brain swelling was calculated as infarct hemisphere volume – non-infarct hemisphere volume.

### Zea-Longa score

The neurobehavioral scores of the P rats were evaluated at

2, 6, 12, and 24 hours after HI, according to the Zea-Longa neurological deficits score (Liu et al., 2019), to determine the establishment of the HI model ($n$ = 20/group). The scoring criteria are as follows: 0 points: behavior is completely normal, without any symptoms of neurological deficit; 1 point: mild neurological deficit, dysfunction in stretching the left forelimb; 2 points: moderate neurological deficit, rats cannot go straight and walk forward because the body continues to turn to the side; 3 points: severe neurological deficit, rats cannot stand and fall to the left when standing; 4 points: Rats cannot walk spontaneously, loss of consciousness.

**Hematoxylin-eosin staining**
To investigate the morphological changes in cortical and hippocampal tissues from P rats, hematoxylin-eosin staining was performed. The extracted tissues were fixed with 4% paraformaldehyde (pH 7.4), embedded in paraffin, and sectioned at a thickness of 5 μm. After transfer to glass slides, the sections were stained with hematoxylin and eosin (Wuxi Jiangyuan Industrial Technology and Trade Corporation, Wuxi, China). Subsequently, the morphological changes in both sham and HI groups were observed under a light microscope (CX40, Shunyu, Ningbo, China). The thickness of the cortex and the hippocampus was measured based on a vertical line perpendicular to the surface of the brain (4.0 mm lateral to the midline and 4.5 mm posterior to the bregma).

**Culture of primary cortical neurons**
Postnatal-day-1 Sprague-Dawley P rats were intragastrically administered 75% alcohol and placed on ice. The cerebral cortexes were harvested and homogenized, followed by isolation with 0.25% trypsin, for 10 minutes, at 37°C, and then eluted with 10% fetal bovine serum. After centrifugation at 15,000 r/min, at room temperature, for 5 minutes, the supernatant was discarded, and the precipitate was resuspended in complete culture medium (Hyclone, Logan, UT, USA), containing high-glucose Dulbecco's modified Eagle medium (DMEM), 10% fetal calf serum, and 1% penicillin-streptomycin solution. Cells were subsequently placed in a 6-well plate containing three coverslips, coated with 50 μg/mL poly-d-lysine and laminin (Sigma-Aldrich, St. Louis, MO, USA), at $5 \times 10^5$ cells/mL, for 4 hours. The medium was replaced with neurobasal medium (Hyclone), containing 2% B27 (Invitrogen, Carlsbad, CA, USA). The culture medium was replaced the following day, and one-half change was performed every 3 days.

**Oxygen-glucose deprivation**
Primary cortical neurons were cultured for 5 days, washed three times with PBS, and then placed into glucose-free medium (Gibco, Shanghai, China) at 37°C. Subsequently, the cells were transferred into a hypoxia chamber, equipped with a compact oxygen controller (Thermo Scientific, Waltham, MA, USA) to maintain the inner concentration of 1% $O_2$, 94% $N_2$, and 5% $CO_2$, at 37°C, for 2 hours. Afterward, cells were reoxygenated by replacing the medium with normal DMEM and incubation in 95% air and 5% $CO_2$, for 24 hours.

**Terminal-deoxynucleotidyl transferase-mediated nick end labeling and Tuj1 staining**
Terminal-deoxynucleotidyl transferase-mediated nick end labeling (TUNEL) and Tuj1 staining were employed to detect neuronal apoptosis and morphological changes in the cortical neurons of P rats. Sections were fixed with 4% paraformaldehyde for 10 minutes, after three rinses with PBS, for 5 minutes each time. After rinsing with PBS again, sections were sealed with PBS, containing 0.1% Triton, in an ice bath, for 2 minutes. The TUNEL reaction mixture was prepared in the dark by combining the enzyme solution and the label solution at a ratio of 1:9, on ice. The specimens were incubated in a dark box, at 37°C, for 1 hour, and 4′,6-diamidino-2-phenylindole (DAPI), containing an anti-fluorescence quencher, was added to the cells, for 3 minutes, at room temperature. Green staining represents TUNEL-positive cells, red staining represents Tuj1-positive cells, and blue staining represents DAPI-positive cells. Positively stained cells were observed under a high-content cell imaging system (Leica, Wetzlar, Germany), and images from each slice were randomly collected.

**Magnetic resonance imaging**
Modern magnetic resonance imaging (MRI) techniques provide excellent anatomical definition and tissue contrast that have led to the identification of specific acute changes in signal intensity and injury patterns associated with HIE (Hochwald et al., 2014). All the T2-weighted imaging (T2WI) tests were performed using a 7.0 T magnetic resonance scanner (Bruker Biospec 70/30, Ettlingen, Germany), with a 75-mm diameter volume coil for radiofrequency pulse transmission and a quadrature surface coil for signal detection, on P rats and F1-rats. During the imaging sessions, the animals were anesthetized as described previously. The body temperatures of all rats were maintained constantly at 37°C, using a heating blanket, and monitored with a rectal temperature probe. T2WI anatomical images were acquired from TS, through a rapid acquisition with spin-echo sequence, using the following parameters: repetition time = 2961.5 ms; echo time = 33 ms; field of view = 3.5 cm × 3.5 cm; matrix = 256 × 256; and slice thickness = 1.0 mm. The total acquisition time was 10 minutes.

**Neurological severity score**
The neurobehavioral conditions of the P rats were assessed at 2 and 3 months after HI, using a 10-point neurological severity score (Lin et al., 2019). The neurological severity score was used to evaluate the abilities of the rats to perform ten different tasks, assessing motor abilities, balance, and alertness. The tasks comprised an exit circle, monopoiesis/hemiparesis, straight walk, startle reflex, seeking behavior, beam balancing, round stick balancing, and beam walking at 1, 2 and 3 cm. A score of one point indicated that none of the tasks could be performed. All neurobehavioral evaluations were performed by two investigators who were blinded to the experimental groups.

**Morris water maze test**

To test the learning and memory abilities of P and F1 rats, the Morris water maze was performed at 2 and 3 months after HI and 3 and 4 months after birth, respectively, as previously described (Chen et al., 2018). The Morris experimental system (Xinruan Information Technology Co., Ltd., Shanghai, China) is composed of a water maze device and an automatic image collection and software analysis system. In this experiment, the Morris water maze device was a 120-cm wide and 56-cm high round pool. The water tank was filled with milky white opaque water, at 18–20°C, to a 30-cm depth. The test was conducted including training and probe trial for 6 consecutive days. The pool was divided into four quadrants, with separate marks that were used to indicate the water entry point in each quadrant. A 10-cm wide cylindrical escape platform was placed 1.5 cm below the water surface and 30 cm away from the wall, in the second quadrant. Furthermore, an automatic camera system was set up over the pool to track the swimming routes of the rats. Before the experiment, the rats were placed in the proper start position, facing the tank wall, and allowed to swim freely for 120 seconds in a separate pool, for acclimation, to reduce their fear response and the generation of feces. A computer tracking program was started when the animal was released into the water. Tracking System SMART 3.0 (Panlab, Spain) was used to record the escape latency and the number of platform crossings.

**Y-maze test**

The Y-maze test was evaluated at 2 and 3 months after HI. The Y-maze device, provided by Shanghai Xinsoft (Shanghai, China), consisted of three arms including initial, wrong, and food arms. The P rats were fasted for 1–2 days, reducing their body weights to 85% of the original weight. In the adaptation period, they were placed in the middle of the apparatus and allowed to move through the maze for approximately 10 minutes, adapted to 2–3 times per day, a total of 1 day, and there is no need to put food (this adaption can be synchronized with the fasting period). During 1-day training period, the food (chocolate or bait) was placed in an arm of the Y maze. The door of the other arm was closed, and the rats were placed in the initial arm to find the food. Finally, the doors of the three arms of the Y-maze were simultaneously opened, with no food; the rats were placed in the starting arm. The arm entries of each rat were observed and recorded and the number of times the rats entered each arm within 5 minutes and the residence time in each arm were recorded (Gastambide et al., 2015).

**Rotarod test**

The rotarod test was performed at 2 and 3 months after HI, as previously described (Mori et al., 2015). Three days before the experiment, adaptive training was performed for P rats, and then the rats were placed on a rotating rod to adapt to the movement on the rod. The rotation speed of the rod was set to 30–35 r/min. The rats were trained for 5–10 minutes per day, for 3 consecutive days. During the following experiment, the rotating rod was set to accelerate from 4 r/min to 40 r/min, within 3 minutes, and the time the rats remained on the rod was recorded. The test was performed continuously, three times a day, and the longest time was marked.

**Detection of brain weight and percentage of brain atrophy**

Two months after HI, the weight of the cerebral hemisphere was measured in P rats. Next, a 2-mm thick brain tissue section was taken 1 mm behind the olfactory bulb and cut into six pieces. These pieces were photographed using a digital camera and traced and analyzed using ImageJ software (Version 1.43u; National Institutes of Health, Bethesda, MD, USA). The percentage of brain atrophy was calculated as (contralateral hemisphere volume − non-infarct ipsilateral hemisphere volume)/contralateral hemisphere volume × 100.

**Body weight detection**

Starting from the first day, when F1 pups were born, the body weight of each rat was measured using an electronic balance (Shanghai Puchun Measure Instrument Co., Ltd., Shanghai, China) at the same time every day for 1 month, and the data were recorded.

**Statistical analysis**

The data were analyzed using SPSS 20.0 software (SPSS, Chicago, IL, USA). All measurement data were expressed as the mean ± SD. Repeated-measures analysis of variance was applied to process the results of the water maze test. Independent-sample Student's $t$-test was applied to all other data. For multiple-group comparisons, analysis of variance, followed by Tukey's *post hoc* test, was used. Student's $t$-test was used to analyze the data between the two groups. A value of $P < 0.05$ was considered to be statistically significant.

## Results

**Neonatal hypoxia and ischemia induce brain infarction and neurological deficits in P rats**

P rats suffered from cerebral ischemia and hypoxia following the ligation of the right common carotid artery and subjection to 8% $O_2$–92% $N_2$ for 2 hours during the neonatal period. The right cerebral hemisphere of the HI group exhibited obvious infarction and brain swelling compared with the sham group, as determined by TTC staining 24 hours after HI ($P < 0.001$; **Figure 1A–D**). In addition, the Zea-Longa scores for the HI group at 2, 6, 12, and 24 hours were significantly increased compared with those for the sham group ($P < 0.05$; **Figure 1E**), peaking at 24 hours.

**Neuronal damage and cell apoptosis increase after HI**

Hematoxylin-eosin staining was applied to observe morphological changes in neurons 7 days after HI. The results directly showed the increased presence of cell cavities and cell nuclei were compressed into the sides of cells in the cortex and hippocampus in the HI group compared with the sham group (**Figure 2A**). Furthermore, to simulate the cerebral

ischemia of neonatal rats *in vitro*, the oxygen-glucose deprivation (OGD) model was established using primary cortical neurons. TUNEL-positive cells in the OGD groups demonstrated increased cellular apoptosis in the OGD group than in the normal group (**Figure 2B**). In addition, Tuj1-positive cells were observed in both the normal and OGD groups. The numbers of neurons and axons observed in the OGD group were lower than those for the normal group (**Figure 2B**).

### Cerebral atrophy and liquefaction in rats after HI
The brain of the HI group showed significant atrophy and liquefaction, resulting in the identification of a tissue defect area compared with the sham group (**Figure 3A**). Correspondingly, the brain weight of the HI group was much lower than that of the sham group (*P* < 0.01; **Figure 3B**). Brains of the HI group were significantly atrophied compared with sham brains (*P* < 0.05; **Figure 3C**).

### HI results in cerebral infarction
Moreover, as demonstrated by the MRI results, the right cerebral hemisphere of HI group rats swelled, infarcted, deliquesced and atrophied in a time-dependent manner. First, severe edema appeared in the right brain of HI group rats, after 24 hours. Then, cerebral liquefaction and atrophy presented at 1, 2, and 3 months (**Figure 4A**). The brain liquefaction ratios at 1, 2, and 3 months were significantly higher than that at 24 hours, and brain atrophy increased largely at 1, 2, and 3 months compared with that at 24 hours (*P* < 0.05; **Figure 4B** and **C**). Hematoxylin-eosin staining further revealed that the thicknesses of the cortex and hippocampus of HI group rats were decreased 2 months after HI. The cortex and hippocampus of the right side of the brain were markedly thinner than those on the left side for HI group rats (*P* < 0.05; **Figure 5A** and **B**).

### HI induces long-term neurological dysfunction in P rats
Behavioral changes were evaluated by Morris water maze, Rotarod, and Y-maze when P rats were two and three months old. In accordance with the neurological severity score test, neurological damage in 2-month-old and 3-month-old HI group rats was much more severe than in similarly aged sham rats (*P* < 0.05; **Figure 6A**). Compared with the sham group, the escape latency in the Morris water maze test was markedly increased in HI group rats aged 2 and 3 months (*P* < 0.05; **Figure 6B**), and the number of platform crossings was substantially decreased in the HI-2m and HI-3m groups (*P* < 0.05; **Figure 6C**). The Y-maze test also showed that error rates (the proportion of times entering the wrong arm) for the HI-2m and HI-3m groups were significantly higher than those for the S-2m and S-3m groups (*P* < 0.05; **Figure 6D** and **F**). The correct rates (the proportion of times entering the food arm) exhibited obvious decreases in the HI groups compared with the sham groups (*P* < 0.05; **Figure 6E** and **G**). The Rotarod test demonstrated that the residence time markedly decreased for the HI-2m and HI-3m groups compared with similarly aged sham groups (*P* < 0.05; **Figure 6H**). Taken together, these results demonstrate

that neurological function was severely damaged in rats subjected to HI.

### No obvious cerebral structural variation in F1 rats
As demonstrated by the MRI results, no significant changes in gross brain structures were observed among HI-F1 rats, including gray matter, white matter and cerebrospinal fluid (**Figure 5C**). During the first 16 days after birth, the daily body weights of HI-F1 rats were mildly heavier than those of sham-F1 rats; however, a significant upward tendency was observed for the daily body weights of Sham-F1 rats at 17, 18, 19, and 20 days compared with those of HI-F1 rats (*P* < 0.05; **Figure 5D**). No significant differences were observed in mortality rates between HI-F1 rats and sham-F1 rats (**Figure 5E**).

### Impaired spatial learning and memory abilities of F1 rats
The Morris water maze test was performed to evaluate behavioral changes in FI rats at 3 and 4 months of age. Using a repeated-measures analysis of variance, the combined data for 5 days were analyzed. The results demonstrated that on different test days, the latency of the HI-F1 group was significantly increased compared with that of the Sham-F1 groups, at 3 and 4 months of age (*P* < 0.05; **Figure 7A** and **B**). The data for each quadrant during the 5-day testing period were analyzed to explore the effects of orientation on latency, which showed measurable increases in the latency of the HI-F1 group for all four quadrants compared with the Sham-F1 group (*P* < 0.05; **Figure 7C** and **D**), for both ages tested. In addition, compared with the Sham-F1 group, the number of platform crossings was substantially decreased in the HI-F1 group (*P* < 0.05; **Figure 7E**).

## Discussion
In this study, after the successful establishment of HIE P model rats, morphological measures of brain growth and development in parental rats with HI-induced brain injuries were significantly different from those in sham rats, whereas the cerebral structural variations were not notable in F1 rats. Furthermore, the results of behavioral tests showed significant differences between the two groups of F1 rats, suggesting that the offspring of parental HI rats exhibited significant learning and memory ability dysfunctions. These data demonstrated that the offspring of parental rats with HI-induced injuries suffered neurodevelopmental defects.

Many animal experiments have confirmed that perinatal brain injury, the primary cause of neonatal HIE, can cause neurological deficits, brain edema, and astrocyte swelling (Li et al., 2015; Liu et al., 2015; Ma et al., 2015) and might impair juvenile recognition memory (Domnick et al., 2015). Early HI brain injuries have been shown to disrupt cortical activity in neonatal rodent models, similar to the findings in human preterm newborns who suffer brain injuries. Studies have shown that neonatal rats experience severe neurological deficits and large numbers of nerve cell deaths during the early stages after cerebral ischemia. In fundamental agreement with these reports, the findings in the current study
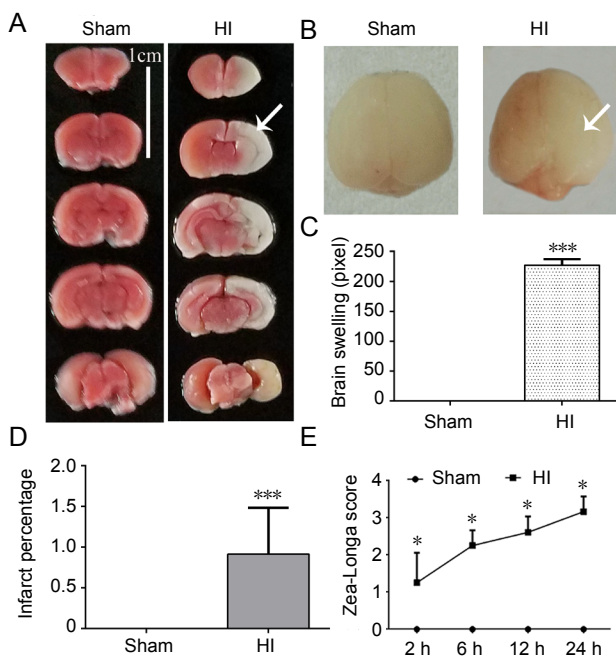
**Figure 1 Successful establishment of parental-generation hypoxia-ischemia (HI) model rats.**
(A) 2,3,5-Triphenyltetrazolium chloride (TTC) staining between sham and HI model rats at 24 hours post-HI. The pale color shows infarction areas (white arrow). Scale bar: 1 cm. The experiment was performed with five slices per brain from each rat in each group. (B) Gross appearance of a normal brain (left) and an infarcted, swollen brain (right). The white arrow indicates brain swelling. (C) Brain swelling from TTC staining, 24 hours after HI ($n = 5$). (D) Infarct percentage (% contralateral), quantified from TTC staining, 24 hours after HI ($n = 5$). (E) Zea-Longa scores at 2, 6, 12, and 24 hours post-HI ($n = 20$). All data are presented as the mean ± SD. ∗$P < 0.05$, ∗∗∗$P < 0.001$, vs. sham group.
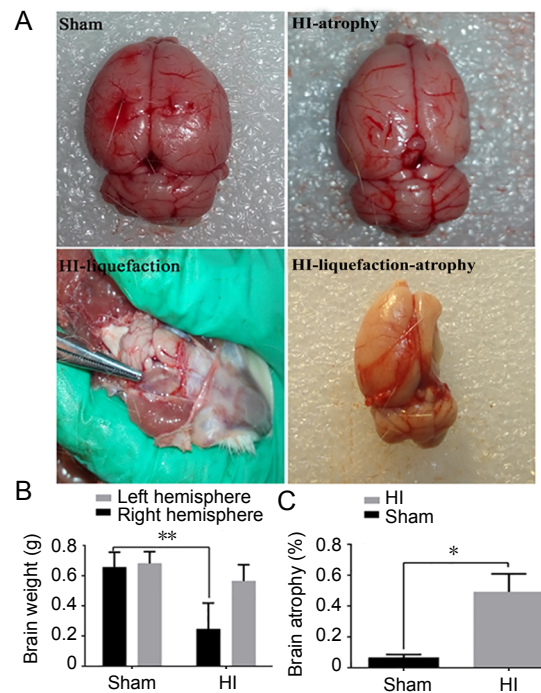


**Figure 3 Atrophy and liquefaction of the brain 2 months after HI.**
(A) Comparison of cerebral appearance between sham rats and HI rats. The damaged brain is outlined in red. (B) Left and right hemisphere weights of sham and HI rats. (C) Percentage of brain atrophy between sham and HI rats. All data are presented as the mean ± SD ($n = 5$). ∗$P < 0.05$, ∗∗$P < 0.01$. HI: Hypoxia-ischemia.
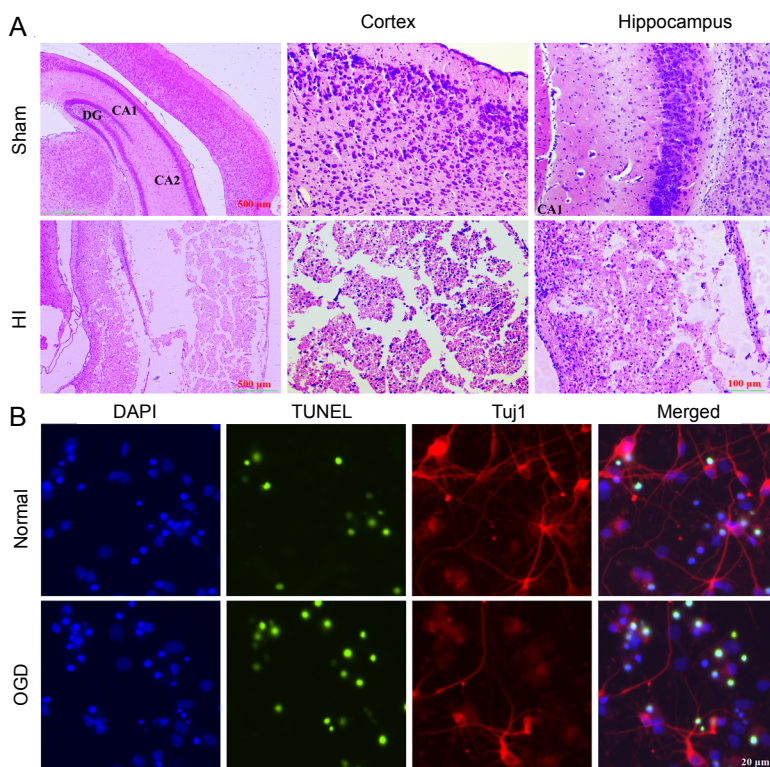


**Figure 2 Morphological changes in neurons after HI.**
(A) Morphology of cells under a light microscope after hematoxylin-eosin staining in the cortex and hippocampus of sham and HI groups, 7 days after HI. On the left, a low-power view (original magnification, 50×) shows the structure of the cortex and hippocampus. Scale bar: 500 μm. In the middle, a high-power view (original magnification, 200×) shows the structure of the cortex. On the right, a high-power view (original magnification, 200×) shows the structure of the CA1 hippocampus. Scale bar: 100 μm. (B) TUNEL and Tuj1 staining of normal and OGD neurons at 24 hours. Scale bar: 20 μm, green for TUNEL-positive cells, red for Tuj1-positive cells, and blue for DAPI-positive cells. ($n = 5$ per group). DAPI: 4′,6-Diamidino-2-phenylindole; HI: hypoxia-ischemia; OGD: oxygen-glucose deprivation; Tuj1: neuronal class III β-Tubulin; TUNEL: terminal-deoxynucleotidyl transferase-mediated nick end labeling.
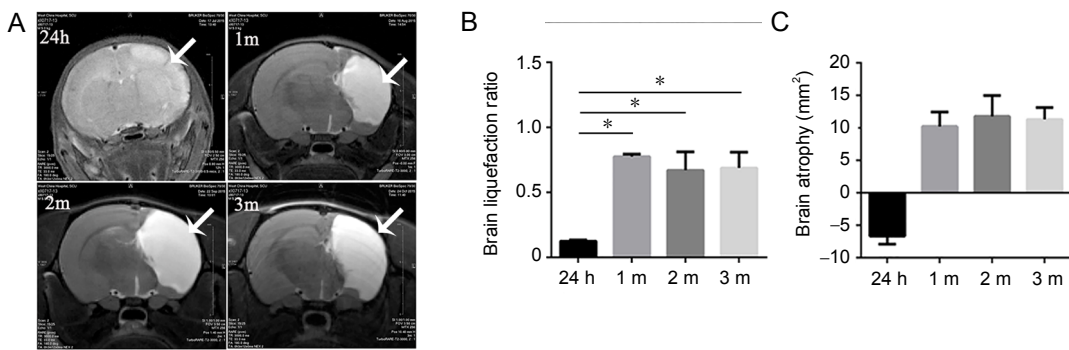
**Figure 4 Changes in cerebral edema, liquefaction, and atrophy in HI rats.**
(A) Magnetic resonance imaging results of HI rats at 24 hours, 1, 2, and 3 months (m). Pale color represents infarction areas (white arrows). (B, C) Brain liquefaction ratio and atrophy at 24 hours, 1, 2, 3, and 4 months. All data are presented as the mean ± SD ($n = 10$). ∗$P < 0.05$. HI: Hypoxia-ischemia.
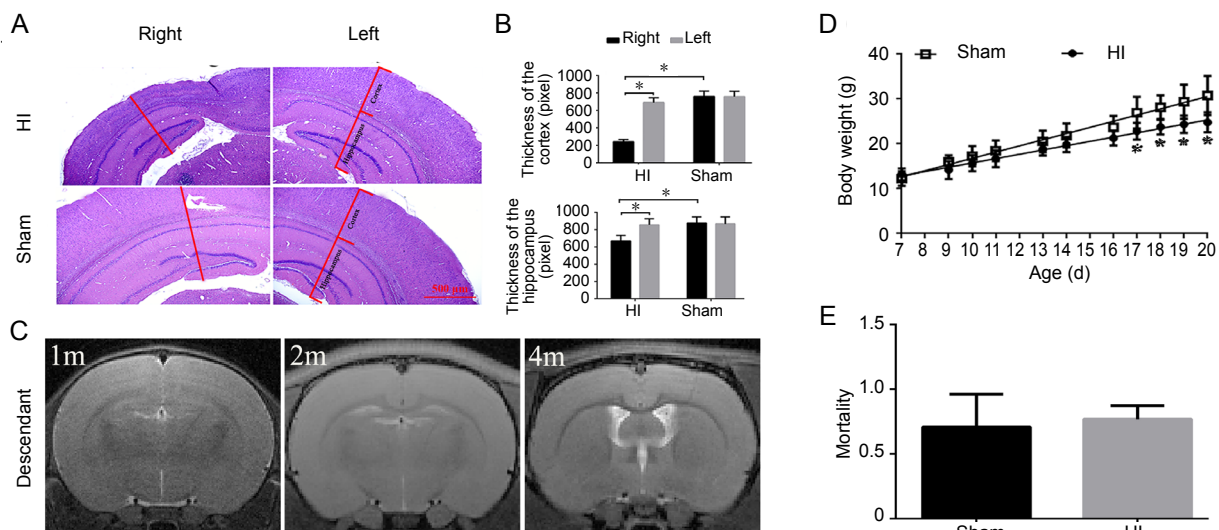


**Figure 5 Morphological cerebral changes of P rats, as well as the cerebral structures and body weights of F1 rats.**
(A) Hematoxylin-eosin staining of the cortex and hippocampus of the HI and sham groups, 2 months (m) after HI. Scale bar: 500 μm. $n = 5$ per group. (B) Quantitative bar chart of the thickness of the cortex and hippocampus on the left and right sides of the brain, 2 months after HI. $n = 5$ per group. (C) Magnetic resonance images of the brain among 1-, 2- and 4-month-old descendants. $n = 10$ per group. (D) Body weight change comparisons between the HI-F1 group and the sham-F1 group, from 2 to 20 days. $n = 10$ per group. (E) Mortality comparison between the HI-F1 group and the sham-F1 group at 20 days. $n = 10$ per group. All data are presented as the mean ± SD. ∗$P < 0.05$, vs. sham group. HI: Hypoxia-ischemia; HI-F1: offspring of HI group; P: parental-generation; Sham-F1: offspring of the sham group.
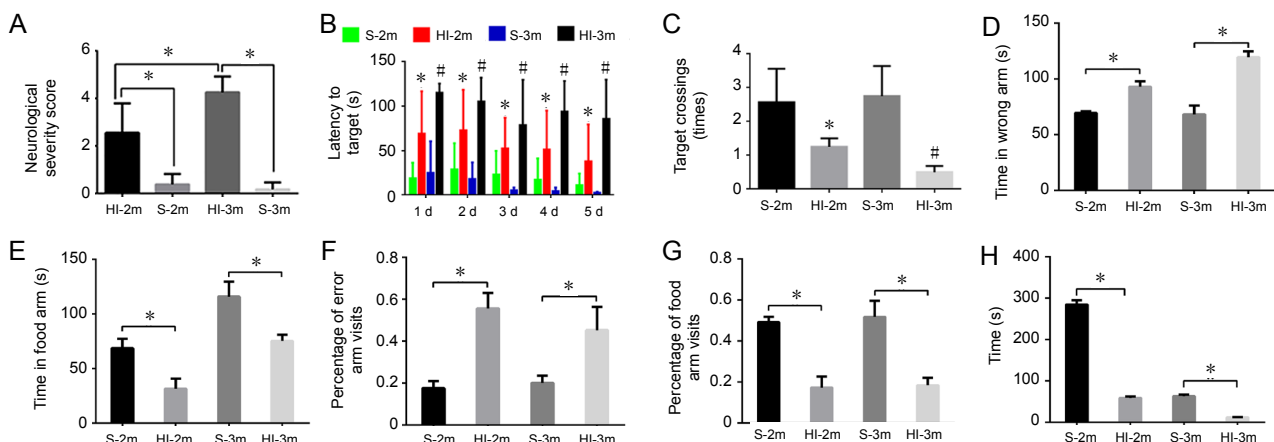


**Figure 6 Morris water maze, Y-maze, and rotarod tests in HI rats after 2 and 3 months.**
(A) Neurological severity score test results in HI-2m, S-2m, HI-3m, and S-3m groups. (B) Escape latencies for these four groups during the Morris water maze test. (C) The number of platform crossings for each of these groups. (D, E) Time spent in the wrong arm and time spent in the food arm during the Y-maze test among these groups. (F, G) Percentage of time spent in the error and food arms four all four groups. (H) Residence time during the rotarod test for all four groups. All data are presented as the mean ± SD ($n = 10$ per group). ∗$P < 0.05$, vs. S-2m group; #$P < 0.05$, vs. S-3m group. HI: Hypoxia-ischemia; m: month; s: sham.
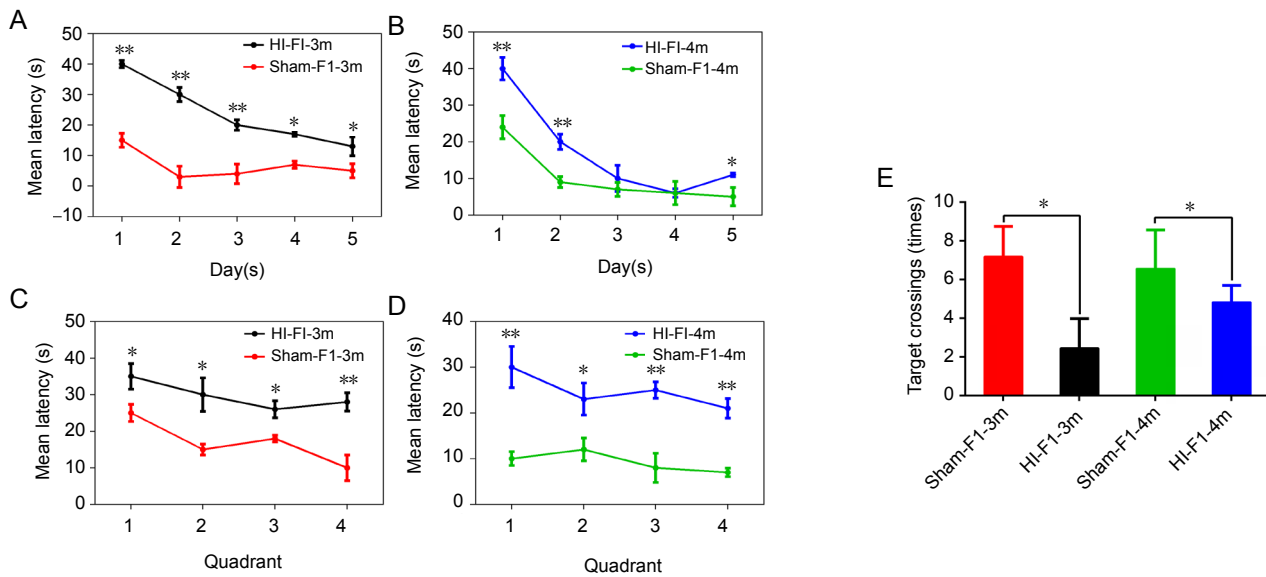
**Figure 7 Spatial learning and memory abilities in F1 rats.**
(A) Mean latency over 5 days in the Sham-F1-3m and HI-F1-3m groups. (B) Mean latency over 5 days in the Sham-F1-4m and HI-F1-4m groups. (C) Latency in each of the four quadrants over 5 days for the Sham-F1-3m and HI-F1-3m groups. (D) Latency in each of the four quadrants over 5 days for the Sham-F1-4m and HI-F1-4m groups. (E) The number of platform crossings compared among the Sham-F1-3m, HI-F1-3m groups, Sham-F1-4m, and HI-F1-4m groups. All data are presented as the mean ± SD ($n = 10$ per group). $*P < 0.05$, $**P < 0.01$, *vs.* Sham-F1-3m or -4m. HI: Hypoxia-ischemia; HI-F1: offspring of HI group; m: month; Sham-F1: offspring of sham group.

demonstrated cortical and hippocampal damage in an HI rat model. In our study, the Zea-Longa scores during the early stage of brain injury indicated that HI rats experienced significant neurological deficits. Simultaneously, TTC staining and MRI showed large areas of infarction in the injured cerebral hemisphere. Furthermore, hematoxylin-eosin staining showed that the sensorimotor cortex of rats was seriously damaged by HI. Moreover, after OGD in rat primary cortical neurons, TUNEL and Tuj1 staining showed increased apoptotic cell numbers and decreased neuronal numbers. In addition, infarction and tissue structure damage could be observed in the hippocampus, which represents the underlying mechanisms of the cognitive impairment observed in adult rats (Ehrenreich, 2017). As expected, behavioral tests performed in rats 2 and 3 months after HI, including neurological severity score, Morris water maze, Y-maze, and rotarod tests, showed that HI rats demonstrated significant memory, attention and executive ability impairments.

The offspring of individuals with mental diseases, such as schizophrenia, depression, and autism, regardless of whether they are caused by abnormal development or environmental factors, are at high risk of developing similar diseases (Green et al., 2018). In addition, several studies have suggested that the children of mothers with mental diseases were more likely to experience variant dysfunctions, such as psychological disorders (Parreco et al., 2018). High-risk offspring had higher rates of subthreshold mania or hypomania, manic, mixed, or hypomanic episodes, and major depressive episodes, and high-risk offspring also had higher rates of attention deficit hyperactivity disorder, disruptive behavior disorders, anxiety disorders, and substance use disorders (Davis et al., 2017). Therefore, to investigate whether the developmental symp-

toms experienced by parental HI patients could impact their children, HI model rats were mated (both parents suffered from HI insults). In accordance with the MRI and Morris water maze test results, no significant differences in cerebral morphology were observed between offspring of HI rats and offspring of normal rats; however, the spatial learning and memory abilities were notably impaired in the offspring of HI rats, indicating that the offspring of parents with HIE may also suffer from neurological dysfunction, which may be associated with genetic factors or other reasons.

Previous studies have shown that mothers with schizophrenia, parental posttraumatic stress disorder, and postnatal depression, in addition to heritable pathogenic genes, have subtle impacts on the behavior of their offspring due to their lack of normal behavioral models and feeding patterns (Schurhoff et al., 2019). In the present study, on the one hand, the genetic acquisition of pathogenic genes may lead to cognitive impairment in offspring. On the other hand, due to HI-induced deficits, HIE-model female rats may be incapable of taking care of their babies and teaching them properly, which may result in the offspring exhibiting similar neurological impairments.

HI injury appears to be sex-specific, and treatments for HI injury are therefore sex-dependent (Demarest et al., 2016; Huang et al., 2016; Waddell et al., 2016). In this study, we only studied the offspring of parental rats with HI insults and found behavioral changes in the offspring of HI rats. Given the notable different sex outcomes following HI injury and the need to exclude pubertal hormonal bias during adolescent social testing, in future studies whether social deficits and biochemical changes are decided by single parents or sex-specific pathways should be clarified.

In conclusion, these findings suggested that the offspring of HI rats have spatial learning and memory ability dysfunctions, which might be associated with parental genes or parental behavioral influences. However, the effects on the hippocampal neurons in the offspring of HI rats and the causes of cognitive impairment have not been further discussed in this study. The underlying causes of behavioral dysfunction require further in-depth investigations in the future. However, our study revealed a new direction for HI research, by investigating offspring, and provided a theoretical reference for clinical treatment, which could be an important indicator of the need to screen offspring for cognitive dysfunction when patients are subjected to HI during the perinatal period.

# References

Chen D, Dixon BJ, Doycheva DM, Li B, Zhang Y, Hu Q, He Y, Guo Z, Nowrangi D, Flores J, Filippov V, Zhang JH, Tang J (2018) IRE1α inhibition decreased TXNIP/NLRP3 inflammasome activation through miR-17-5p after neonatal hypoxic-ischemic brain injury in rats. J Neuroinflammation 15:32.

Davies A, Wassink G, Bennet L, Gunn AJ, Davidson JO (2019) Can we further optimize therapeutic hypothermia for hypoxic-ischemic encephalopathy?. Neural Regen Res 14:1678-1683.

Davis AM, Rubinstein TB, Rodriguez M, Knight AM (2017) Mental health care for youth with rheumatologic diseases - bridging the gap. Pediatr Rheumatol Online J 15:85.

Demarest TG, Schuh RA, Waddell J, McKenna MC, Fiskum G (2016) Sex-dependent mitochondrial respiratory impairment and oxidative stress in a rat model of neonatal hypoxic-ischemic encephalopathy. J Neurochem 137:714-729.

Domnick NK, Gretenkord S, De Feo V, Sedlacik J, Brockmann MD, Hanganu-Opatz IL (2015) Neonatal hypoxia-ischemia impairs juvenile recognition memory by disrupting the maturation of prefrontal-hippocampal networks. Exp Neurol 273:202-214.

Driscoll DJO, Felice VD, Kenny LC, Boylan GB, O'Keeffe GW (2018) Mild prenatal hypoxia-ischemia leads to social deficits and central and peripheral inflammation in exposed offspring. Brain Behav Immun 69:418-427.

Ehrenreich H (2017) The impact of environment on abnormal behavior and mental disease: To alleviate the prevalence of mental disorders, we need to phenotype the environment for risk factors. EMBO Rep 18:661-665.

Ferriero DM (2004) Neonatal brain injury. N Engl J Med 351:1985-1995.

Galinsky R, Davidson JO, Dean JM, Green CR, Bennet L, Gunn AJ (2018) Glia and hemichannels: key mediators of perinatal encephalopathy. Neural Regen Res 13:181-189.

Gastambide F, Taylor AM, Palmer C, Svard H, Karjalainen M, Janhunen SK, Tricklebank M, Bannerman DM (2015) Alterations in spatial memory and anxiety in the MAM E17 rat model of hippocampal pathology in schizophrenia. Psychopharmacology (Berl) 232:4099-4112.

Getahun D, Fassett M, Wing D, Jacobsen S (2013) 704: Association between perinatal ischemic-hypoxic conditions and autism spectrum disorder. Am J Obstet Gynecol 208:S296.

Graham EM, Ruis KA, Hartman AL, Northington FJ, Fox HE (2008) A systematic review of the role of intrapartum hypoxia-ischemia in the causation of neonatal encephalopathy. Am J Obstet Gynecol 199:587-595.

Green MJ, Kariuki M, Dean K, Laurens KR, Tzoumakis S, Harris F, Carr VJ (2018) Childhood developmental vulnerabilities associated with early life exposure to infectious and noninfectious diseases and maternal mental illness. J Child Psychol Psychiatry 59:801-810.

Hochwald O, Jabr M, Osiovich H, Miller SP, McNamara PJ, Lavoie PM (2014) Preferential cephalic redistribution of left ventricular cardiac output during therapeutic hypothermia for perinatal hypoxic-ischemic encephalopathy. J Pediatr 164:999-1004.e1.

Huang HZ, Wen XH, Liu H (2016) Sex differences in brain MRI abnormalities and neurodevelopmental outcomes in a rat model of neonatal hypoxia-ischemia. Int J Neurosci 126:647-657.

Kawarai Y, Tanaka H, Kobayashi T, Shozu M (2018) Progesterone as a postnatal prophylactic agent for encephalopathy caused by prenatal hypoxic ischemic insult. Endocrinology 159:2264-2274.

Kurinczuk JJ, White-Koning M, Badawi N (2010) Epidemiology of neonatal encephalopathy and hypoxic-ischaemic encephalopathy. Early Hum Dev 86:329-338.

Leviton A, Nelson KB (1992) Problems with definitions and classifications of newborn encephalopathy. Pediatr Neurol 8:85-90.

Li SH, Sun HT, Wang YM, Wei ZJ (2015) Therapeutic effect of acupuncture treatment on ischemic hypoxic neonate rats with cerebral palsy. Zhongguo Ying Yong Sheng Li Xue Za Zhi 31:473-476.

Lin SJ, Zhang YJ, Lin JH, Zhang YM, Zhu MM, Zhang YQ, Pu L, Chen SL, Chen WH, Cheng SB (2019) Effect of acupuncture intervention on neurological function, cerebral microglia activation and secondary nerve damage in traumatic brain injury rats. Zhen Ci Yan Jiu 44:19-24.

Liu S, Zhu S, Zou Y, Wang T, Fu X (2015) Knockdown of IL-1beta improves hypoxia-ischemia brain associated with IL-6 up-regulation in cell and animal models. Mol Neurobiol 51:743-752.

Liu XH, Bi HY, Cao J, Ren S, Yue SW (2019) Early constraint-induced movement therapy affects behavior and neuronal plasticity in ischemia-injured rat brains. Neural Regen Res 14:775-782.

Ma Z, Yan SZ, Wang XL, Chen W, Cao XY, Dong P, Zhao YS (2015) Effects of umbilical cord mononuclear cells transplantation combined with hyperbaric oxygen therapy on hypoxic-ischemic brain damage in neonatal rats. Zhongguo Dang Dai Er Ke Za Zhi 17:736-740.

Mori M, Matsubara K, Matsubara Y, Uchikura Y, Hashimoto H, Fujioka T, Matsumoto T (2015) Stromal cell-derived factor-1alpha plays a crucial role based on neuroprotective role in neonatal brain injury in rats. Int J Mol Sci 16:18018-18032.

Mwaniki MK, Atieno M, Lawn JE, Newton CR (2012) Long-term neurodevelopmental outcomes after intrauterine and neonatal insults: a systematic review. Lancet 379:445-452.

Parreco J, Alawa N, Rattan R, Tashiro J, Sola JE (2018) Teenage trauma patients are at increased risk for readmission for mental diseases and disorders. J Surg Res 232:415-421.

Sasaoka N, Kawaguchi M, Kawaraguchi Y, Nakamura M, Konishi N, Patel H, Patel PM, Furuya H (2009) Isoflurane exerts a short-term but not a long-term preconditioning effect in neonatal rats exposed to a hypoxic-ischaemic neuronal injury. Acta Anaesthesiol Scand 53:46-54.

Schurhoff F, Fond G, Berna F, Bulzacka E, Godin O, Boyer L, Misdrahi D, Andrianarisoa M, Brunel L, Coulon N, Aouizerate B, Capdevielle D, Chereau I, D'Amato T, Dubertret C, Dubreucq J, Faget C, Gabayet F, Mallet J, Rey R, et al. (2019) The 10-year findings from the FondaMental Academic Center of Expertise for Schizophrenia (FACE-SZ): Review and recommendations for clinical practice. Encephale 45:9-14.

Selway LD (2010) State of the science: hypoxic ischemic encephalopathy and hypothermic intervention for neonates. Adv Neonatal Care 10:60-66; quiz 67-68.

Vannucci RC, Perlman JM (1997) Interventions for perinatal hypoxic-ischemic encephalopathy. Pediatrics 100:1004-1014.

Vannucci RC, Connor JR, Mauger DT, Palmer C, Smith MB, Towfighi J, Vannucci SJ (1999) Rat model of perinatal hypoxic-ischemic brain damage. J Neurosci Res 55:158-163.

Vannucci SJ, Hagberg H (2004) Hypoxia-ischemia in the immature brain. J Exp Biol 207:3149-3154.

Wachtel EV, Hendricks-Munoz KD (2011) Current management of the infant who presents with neonatal encephalopathy. Curr Probl Pediatr Adolesc Health Care 41:132-153.

Waddell J, Hanscom M, Shalon Edwards N, McKenna MC, McCarthy MM (2016) Sex differences in cell genesis, hippocampal volume and behavioral outcomes in a rat model of neonatal HI. Exp Neurol 275 Pt 2:285-295.